Kovove Mater. 50 2012 69–73
DOI: 10.4149/km_2012_2_69

Influence of corrosive solution temperature on the SCC behavior of the AISI 310 and AISI 316 stainless steels rolled plates

J. C. Fernandes[1], E. O. Correa[1*] , M. L. N. M. Melo[1], R. P. Barbosa[2]

[1] *Instituto de Engenharia Mecânica, Universidade Federal de Itajuba, Av BPS, 1303, Itajuba, Minas Gerais, Brazil 37500-903, Brazil*
[2] *Aperam South America, Timoteo, Minas Gerais, Brazil*

Received 14 June 2011, received in revised form 20 July 2011, accepted 26 July 2011

Abstract

In this study, the influence of the corrosive solution temperature on the stress corrosion cracking (SCC) behavior of the AISI 310 and AISI 316 stainless steels rolled plates using a constant load method was investigated. For the AISI 316, the relationship between the time to failure and the test temperature fell into a linear function for the temperatures from 143 to 152 °C and an exponential function for the temperatures from 132 to 143 °C. These regions are considered to correspond to a SCC-dominated region and a hydrogen embrittlement--dominated region. Microstructural analyses showed that in the SCC-dominated region the fracture mode was transgranular, but it was intergranular in the hydrogen embrittlement--dominated region. For the AISI 310 steel, the relationship between the time to failure and the test temperature fell into a linear function for the temperatures from 132 to 152 °C. The fracture mode was transgranular for all temperatures, which strongly indicated that this steel showed SCC only.

K e y w o r d s: stress corrosion cracking, temperature, austenitic stainless steels

1. Introduction

The stress corrosion cracking (SCC) susceptibility of austenitic stainless steels in chloride has been extensively investigated using various methods [1–3]. However, there is no general cracking mechanism that explains precisely the stress corrosion phenomenon, that is, each specific material--environment combination presents its particularities.

The SCC cracking mechanisms for austenitic stainless steels can be grouped in anodic and cathodic depending on the main cause of the cracking propagation either the active path dissolution of the material at the crack tip, passive film rupture, or fracture associated to the presence of diffuse hydrogen in the crystalline structure (hydrogen embrittlement) [4].

According to [5], depending on the austenitic stainless steel type, the environment and the temperature, a determined cracking mechanism may change or not show up, which influences directly the cracking propagation mode and, consequently, the SCC resistance of these steels.

It is reported that the austenitic stainless steel AISI 316, differently from the type 310, undergoes phase transformation from γ (austenite) $\rightarrow \alpha'$ (martensite) due to applied stress or hydrogen charging [6]. It is worthwhile mentioning that phase martensite is directly related to the brittle fracture and predominance of intergranular stress corrosion cracks in this austenitic stainless steel.

Therefore, the diffusion of hydrogen into the material together with the presence of stress induced martensite may influence significantly the SCC behavior of these austenitic stainless steels [7].

Also, considering that the microstructure and the corrosion reaction kinetics affect considerably the susceptibility of the austenitic stainless steels in a corrosive environment, this study aims to investigate the influence of the corrosive solution temperature on the SCC susceptibility of the AISI 316 and AISI 310 austenitic stainless steels rolled plates.

*Corresponding author: tel.: +55-35-36291298; fax: +55-35-36291148; e-mail address: ecotoni@unifei.edu.br

Table 1. Chemical composition of the austenitic stainless steels studied (wt.%)

Material	C	Si	Mn	Cu	Cr	Ni	Mo	Fe
AISI 316	0.03	0,5	1.4	0.01	16	9	2	Bal
AISI 310	0.05	0.5	1.5	0.2	24	18.8	0.2	Bal

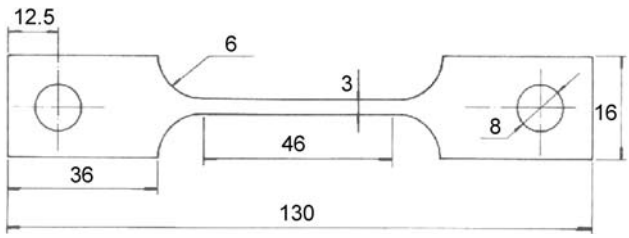

Fig. 1. Smooth specimen geometry (dimensions in mm).

2. Experimental procedure

A constant-load lever arm apparatus was used to evaluate the influence of the temperature on the susceptibility to SCC of the AISI 316 and AISI 310 austenitic stainless steel specimens in aerated boiling $MgCl_2$ test solution. *In order to obtain the test temperatures studied (from 132 to 152°C), the aqueous $MgCl_2$ solution concentration varied from 30 to 45 wt.% of $MgCl_2$.* Chemical composition (wt.%) of the stainless steels used is shown in Table 1.

3 mm thick smooth rectangular tensile specimens, as can be seen in Fig. 1, obtained from the cold rolled plates, were used for the SCC tests. The preparation of the specimens was in accordance with ASTM G58 and ASTM E8 standards.

After polishing to 1000 grit emery paper and degreasing with acetone and washing with distilled water, specimens were put in a glass vessel in which the test solution was placed. The glass vessel was coupled to a reflow condenser so that all measurements were monitored continuously under closed-circuit conditions. Sealing between glass vessel and specimen was done by silicon rubbers. The tests were conducted at a tensile load corresponding to the nominal stress level of 300 MPa, which was associated with SCC dominated failure in this type of environment for austenitic stainless steel. Time-to-failure was the SCC parameter evaluated.

The SCC fracture mode was studied on fully ruptured SCC specimens. Starting from the tested specimens, 20 mm thickness specimens were removed and polished to diamond finish, and optical micrographs were taken after etching.

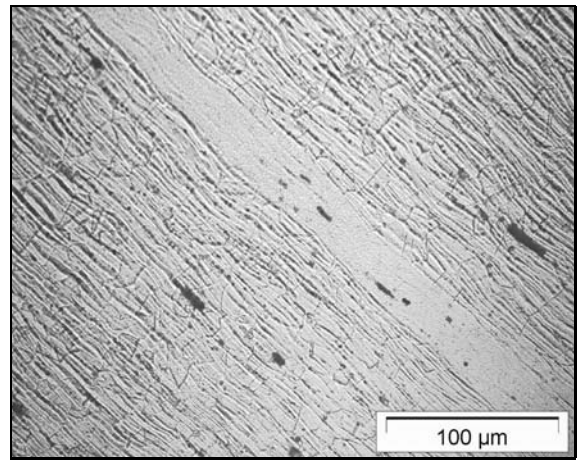

Fig. 2. Microstructure of AISI 316 stainless steel (as rolled).

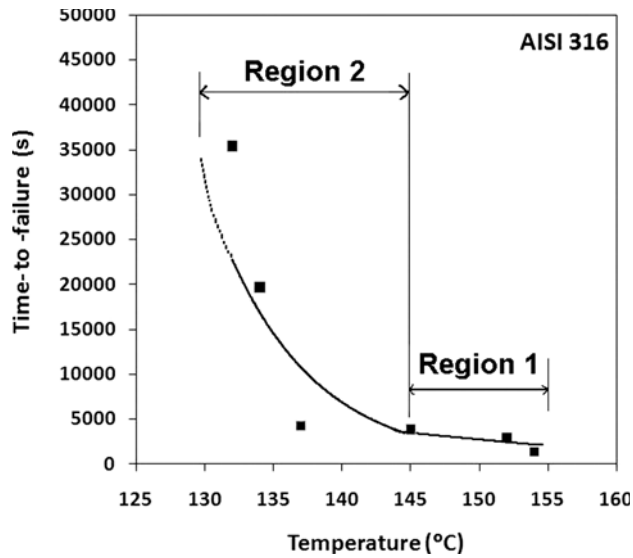

Fig. 3. Time to failure versus test temperature for AISI 316 stainless steel.

3. Results and discussion

3.1. AISI 316 stainless steel

Figure 2 shows the microstructure of the cold rolled AISI 316 stainless steel. Deformed grains in the rolling direction can be noted. Although this steel presents a duplex structure comprised of austenite and delta-ferrite, the presence of delta-ferrite in the austenite grain boundaries is not observed clearly. This is attributed to the fact that during the final cold rolling stages, the metastable delta ferrite is dissolved in the matrix transforming to austenite.

Figure 3 depicts the time-to-failure versus the solution temperature for the AISI 316 stainless steel ob-

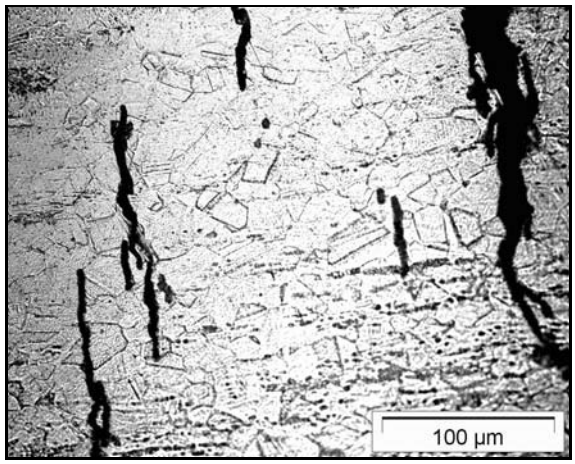

Fig. 4. Transgranular cracking for type 316 in the region 1: 148 °C.

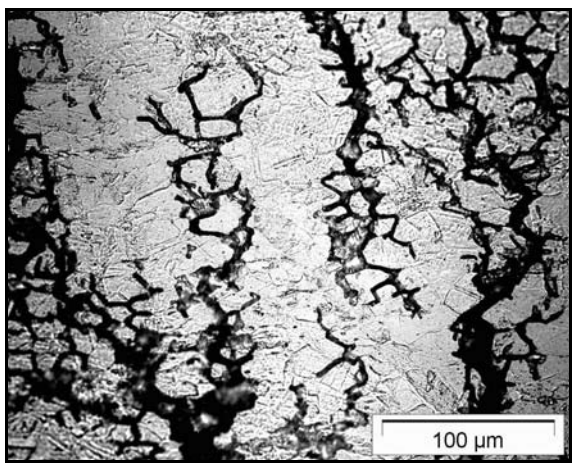

Fig. 5. Intergranular cracking for type 316 in the region 2: 132 °C.

tained from the SCC tests. For this steel, the relationship between the time to failure and temperature falls in a linear function (straight line), shown as region 1, from 143 to 152 °C. However, for lower solution temperatures (132 to approximately 143 °C), shown as region 2, the function deviates considerably from the linearity.

According to several researchers [2–4], the presence of these two regions in the graph indicates that (1) there were two SCC mechanisms and (2) a change of the predominant SCC mechanism occurred as the solution temperature increased.

In order to identify modification in the SCC fracture mode that evidenced the presence of these two mechanisms as a function of the temperature, microstructural analyses of the materials tested in temperatures inside both regions were carried out.

Figures 4 and 5 show stress corrosion cracks in specimens tested in region 1 and 2, respectively.

It can be seen from Fig. 4 that the fracture mode in the region 1 is predominantly transgranular, which is characterized by the occurrence of the crack propagation under a relatively straight and smooth cracking path through the middle of the grains. It can also be noted that the lower amount of SCC cracks nucleated in the bulk material in this region.

On the other hand, it can be seen from Fig. 5 that the fracture mode in the region 2 is predominantly intergranular, which is characterized by the occurrence of the crack propagation under a nonplanar and tortuous cracking path along the austenitic grain boundaries. It can also be noted that the higher amount of SCC cracks nucleated in the bulk material in this region.

According to Nishimura et al. [8], the predominance of transgranular cracks in the region 1 indicates that the dominant SCC mechanism is the active path dissolution of the material at the crack tip. Additionally, as can be seen in Fig. 3, the time to fracture in this region is considerably lower than that observed in the region 2, which shows the much more deleterious effect of this SCC mechanism in the material.

Concerning to the region 2, the predominance of intergranular cracks may be attributed to the hydrogen embrittlement mechanism. The occurrence of this cracking mechanism in the AISI 316 steel is due to the fact that the austenite in its microstructure is metastable and it is very susceptible to stress induced martensite formation. This martensite, formed along the austenite grain boundaries, increases the diffusion of hydrogen produced by the electrochemical reactions at the metal surface. In addition, the martensitic structure has a high hydrogen diffusivity coefficient and lower hydrogen solubility limit compared to those of the austenite, which may explain the crack preferential path is intergranular through the martensite structure facilitated by the higher diffusion rates of hydrogen [3, 9].

It is also worthwhile mentioning that at high temperatures (region 1), the corrosion rate is much higher than the corrosion rate at low temperatures (region 2). As a result, the metal dissolution at the crack tip is faster than the hydrogen diffusion to the crystal structure and this is the main reason to the predominance of the SCC mechanism in the region 1 [10].

3.2. AISI 310 stainless steel

Figure 6 shows the microstructure of the cold rolled AISI 310 stainless steel. The deformed polygonal austenite grains and the presence of deformation twins inside several grains can be noted. This steel presents a microstructure similar to the AISI 316 comprised of austenite and delta-ferrite. Similarly to the AISI 316 stainless steel, the presence of delta ferrite in the austenite grain boundaries is not easily detected.

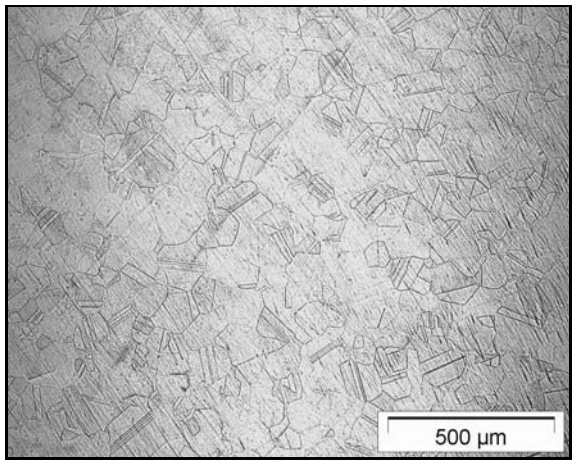

Fig. 6. Microstructure of AISI 310 stainless steel (as rolled).

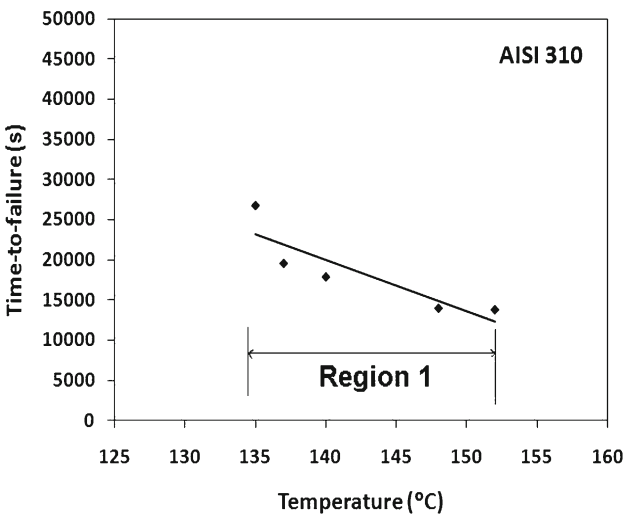

Fig. 7. Time to failure versus test temperature for AISI 310 stainless steel.

Figure 7 depicts the time-to-failure versus the solution temperature for the AISI 310 stainless steel obtained from the SCC tests. For this steel, the relationship between the time to failure and temperature falls in a linear function (straight line) for all temperatures in the range studied (132 to 152 ℃). This indicates that, differently from the AISI 316 steel, this steel does not show a cracking mechanism changing as the temperature increases. Additionally, it can be seen from Fig. 7 that the times to fracture for the AISI 310 are higher than those for the AISI 316, which demonstrates that this steel is more resistant to SCC.

In order to verify whether the cracking fracture mode is really the same for all temperatures, microstructural analyses of the AISI 310 steel for several temperatures from 132 to 152 ℃ were also carried out.

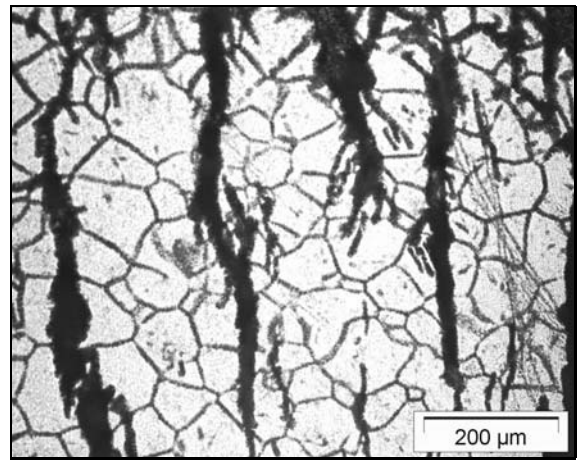

Fig. 8. Transgranular cracking for type 310 at the temperature of 152 ℃.

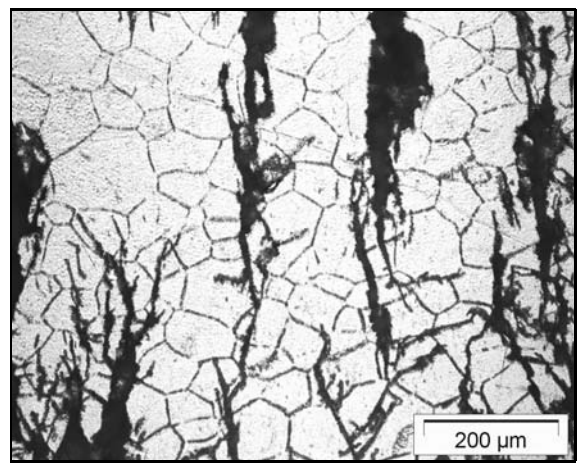

Fig. 9. Transgranular cracking for type 310 at the temperature of 140 ℃.

Figures 8, 9 and 10 show stress corrosion cracks in AISI 310 steel specimens tested in three different temperatures.

It can be noted clearly from figures that the cracking fracture mode was predominantly transgranular once the crack propagation occurred under a relatively straight and smooth cracking path through the middle of the grains. According to several researchers [4–7], this indicates that there was the presence of the SCC mechanism only and the absence of the hydrogen embrittlement mechanism in lower temperatures.

This may be attributed to the fact that the austenite in the microstructure of AISI 310 steel is much more stable once this steel contains much higher Ni content (austenite stabilizer) in its chemical composition compared to the AISI 316 steel. As a result, this steel practically did not present stress induced martensite in its microstructure, which reduces significantly the hydrogen diffusion on the metal surface

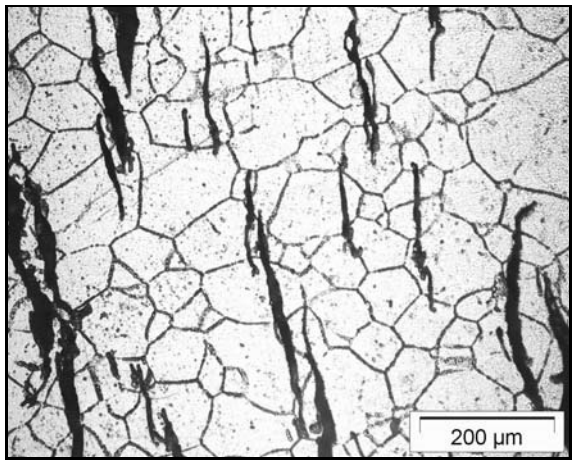

Fig. 10. Transgranular cracking for type 310 at the temperature of 135 °C.

into the structure and, consequently, the susceptibility of the material to hydrogen embrittlement [6–8].

It is worthwhile mentioning that increasing the amount of stress induced martensite content in the structure increases the susceptibility of the material to hydrogen embrittlement [10]. According to Eliezer et al. [11], the most probable SCC mechanism of the AISI 310 steel is the passive film rupture.

4. Conclusions

a) Using an SCC constant load method, the effect of the temperature on SCC of the austenititic stainless steel AISI 316 was evaluated. For this steel, two regions were observed: one with the predominance of the SCC failure mechanism for temperatures from 143 to 152 °C, and other with the predominance of the hydrogen embrittlement failure mechanism for temperatures from 132 to approximately 143 °C.

b) It was observed by microstructural evaluation that the predominant cracking fracture mode for the SCC mechanism was transgranular and that the predominant cracking fracture mode for the hydrogen embrittlement was intergranular.

c) The reason for the intergranular fracture mode for the AISI 316 stainless steel in lower temperatures may be attributed to the formation of stress induced martensite at the austenite grain boundaries.

d) The effect of the temperature on SCC behavior of the austenitic stainless steel AISI 310 is quite different from that observed for the AISI 316 steel. For this steel, the SCC failure mechanism for all temperatures (from 132 to 152 °C) was observed only. The cracking mechanism was predominantly transgranular at test temperatures and no intergranular cracking behavior was observed, probably, due to the absence of martensite transformation. Furthermore, the AISI 310 steel showed longer times to fracture compared to the AISI 316 steel, which indicates that this steel exhibits a higher SCC resistance.

Acknowledgements

The authors acknowledge the Brazilian government agencies FAPEMIG and CNPq for the financial support.

References

[1] HOAR, T. P.—WEST, J. M.: Proc. Roy. Soc., *A268*, 1962, p. 304. http://dx.doi.org/10.1098/rspa.1962.0142
[2] NISHIMURA, R.—MAEDA, Y.: Corrosion Science, *46*, 2004, p. 769. http://dx.doi.org/10.1016/j.corsci.2003.08.001
[3] NISHIMURA, R.—MAEDA, Y.: Corrosion Science, *45*, 2003, p. 1847. http://dx.doi.org/10.1016/S0010-938X(03)00002-7
[4] NAKAYAMA, T.—TAKANO, M.: Corrosion, *42*, 1986, p. 10.
[5] Metals Handbook. Vol. 13. Metals Park, Ohio, ASM International 1987.
[6] NARITA, N.—ALTSTETTER, C. J.—BIRNBAUM, H. K.: Metallurgical and Materials Transactions A, *13*, 1982, p. 1355.
[7] SCULLY, J. C.: In: ICCM Proceedings of the 1975 International Conference on Composite Materials. New York, Metallurgical Society of AIME 1976, p. 129.
[8] NISHIMURA, R.—SULAIMAN, A.—MAEDA, Y.: Corrosion Science, *45*, 2003, p. 465. http://dx.doi.org/10.1016/S0010-938X(02)00132-4
[9] BRIANT, C. L.: Metallurgical and Materials Transactions A, *10*, 1979, p. 181. http://dx.doi.org/10.1007/BF02817627
[10] HANNINEN, H.—HAKARAINEN, T.: Corrosion, *36*, 1980, p. 47.
[11] ELIEZER, D.—CHAKRAPANI, D. G.—ALTSTETTER, C. J.—PUGH, E. N.: Metallurgical and Materials Transactions A, *10*, 1979, p. 935.